DE GRUYTER OPEN

Archives of Hydro-Engineering and Environmental Mechanics
Vol. 65 (2018), No. 2, pp. 73–90
DOI: 10.1515/heem-2018-0006

Influence of Wave Shape on Sediment Transport in Coastal Regions

Rafał Ostrowski

Institute of Hydro-Engineering, Polish Academy of Sciences, ul. Kościerska 7, 80-953 Gdańsk, Poland
e-mail: rafal.o@ibwpan.gda.pl

(Received September 05, 2018; revised November 11, 2018)

Abstract

The paper deals with the influence of the wave shape, represented by water surface elevations and wave-induced nearbed velocities, on sediment transport under joint wave-current impact. The focus is on the theoretical description of vertically asymmetric wave motion and the effects of wave asymmetry on net sediment transport rates during interaction of coastal steady currents, namely wave-driven currents, with wave-induced unsteady free stream velocities. The cross-shore sediment transport is shown to depend on wave asymmetry not only quantitatively (in terms of rate), but also qualitatively (in terms of direction). Within longshore lithodynamics, wave asymmetry appears to have a significant effect on the net sediment transport rate.

Key words: wave shape, nearbed free stream velocities, wave-driven currents, cross-shore sediment transport, longshore sediment transport

1. Introduction

Many coastal engineering problems are associated with changes in the sea bed profile. Investigations of this evolution are partly related to search for the origin of bars and theoretical description of their migration. Besides, the knowledge of sea bed dynamics makes it possible to accurately predict changes in the shoreline position. Conventionally, coastal morphodynamics are modelled theoretically by means of the spatial variability of net sediment transport rates. Models of evolution of the sea bed and the shoreline are highly sensitive to the qualitative and quantitative variability of net sediment transport. Hence the need for its precise determination.

For practical reasons, one traditionally distinguishes between cross-shore and longshore sediment transport in coastal zones. The cross-shore motion of sediments is caused by waves interacting with a wave-driven current called undertow. The undertow can be modelled by the classic approach of Longuet-Higgins, in which the momentum equation in the cross-shore direction, integrated over water depth and wave period, describes the equilibrium between the derivative of the radiation stress

($\partial S_{xx}/\partial x$) and the spatial change in the free surface slope (resulting from phenomena known as the set-down and the set-up, seawards and landwards from the wave breaking point, respectively). On the other hand, these two components of the momentum equation are in local imbalance at various depths in the water column. This is because the component containing the water slope is constant over water depth, whereas the radiation stress S_{xx} is variable as a result of the decrease in wave orbital velocities towards the sea bed. This imbalance, which is particularly significant in the surf zone, is the driving force behind the resultant offshore current, known as the undertow. In addition, there is an onshore discharge of water between the wave crest and trough, related to the so-called wave drift (or Stokes drift). As a result of the continuity equation, this onshore current requires compensation in the form of undertow, see Szmytkiewicz (1996, 2002a, 2002b) for more details. Interaction between waves and the undertow gives rise to resultant sediment transport, the direction of which is principally dependent on a very delicate imbalance between the undertow and onshore nearbed streaming caused by the vertical asymmetry of the wave shape, see Ostrowski (2002, 2003, 2004). Vertically asymmetric waves are characterized by short high crests and long shallow troughs.

The longshore current, generated by waves obliquely approaching the shore and breaking in the surf zone, is a driving force of the longshore transport of sediment. Part of the energy (and momentum) of breaking waves is converted to a steady flow. A precise description of this longshore wave-induced flow, similarly as in the case of undertow, has become possible due to the development of the radiation stress concept in the late 1960s. Since then, a number of studies have been published in which the longshore flow is described as being generated by the S_{xy} component of the radiation stress. A theoretical model of longshore currents in a multi-bar coastal zone (for multiple wave breaking), along with a comparison of the model results with experimental data, is presented in a book by Szmytkiewicz (2002a). In most theoretical models, the longshore transport is assumed to depend on a combined wave and current motion. This combined flow of water gives rise to a coupled bed shear stress, which is a driving force for sand movement along the shore. The longshore sediment transport rate has been shown to depend distinctly on wave asymmetry, see Ostrowski and Szmytkiewicz (2006).

Sediment transport characteristics are very sensitive to hydrodynamic phenomena. The relationships between driving forces and ultimate morphological responses are highly non-linear and ought to be thoroughly investigated. As proved by Ostrowski (2002, 2003, 2004) for the cross-shore domain, even a minor change in proportions between the wave asymmetry effects and the undertow can have an enormous impact on the net sediment transport rate in both quantitative and qualitative terms. For the longshore domain, Ostrowski and Szmytkiewicz (2006) have shown that the wave asymmetry effects influence the net sediment transport in a quantitative sense only. In view of the above, it appears obvious that one can encounter research uncertainties on these fronts. The objective of the present paper is to analyse the wave shape in the context of sediment motion under waves and wave-driven currents.

2. Nearbed Wave-induced Free Stream Velocities

Despite the random (irregular) character of sea waves, their description makes extensive use of the theories of regular surface waves. Basic wave parameters comprise the wave height (H), period (T) and length (L), as well as the water depth (h) at the given location. Notation used in wave theories is presented in Fig. 1, which shows a distinctly asymmetric wave, with a short high crest and a long shallow trough.

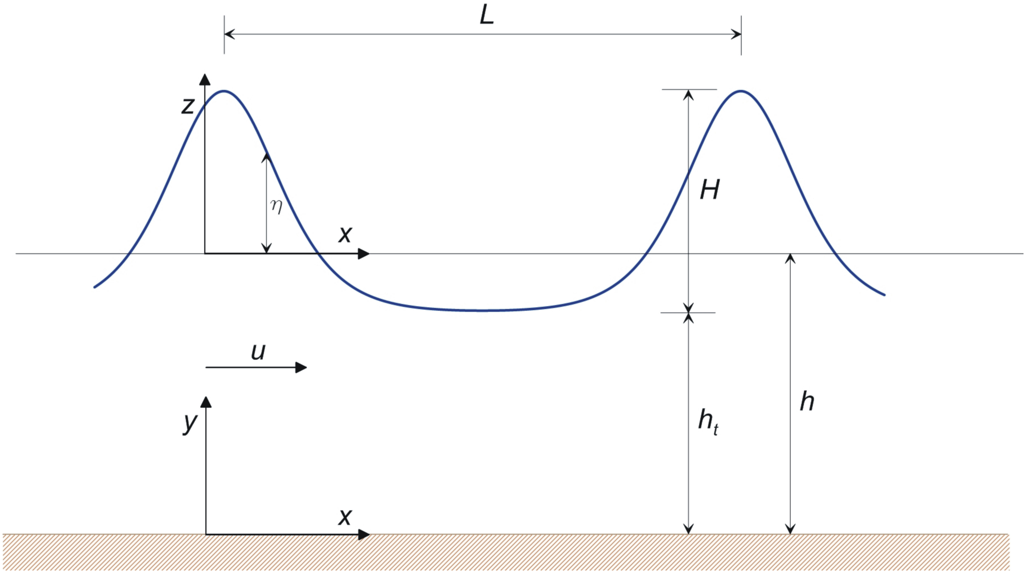

Fig. 1. Notation in wave theories

The linear wave theory, also known as the sinusoidal wave theory, is one of the fundamental descriptions of regular waves. Its name refers to the wave profile, which has a sinusoidal shape. This occurs only in the case of waves having small heights and lengths, propagating over relatively large depths, see Massel (1992). The sinusoidal wave theory is often used in engineering practice, even beyond the scope of its validity. The relationship between the wave period T and length L in the theory of sinusoidal waves is expressed by the following equation, called a dispersion relationship:

$$\left(\frac{2\pi}{T}\right)^2 = g\left(\frac{2\pi}{L}\right)\tanh\left[\left(\frac{2\pi}{L}\right)h\right], \tag{1}$$

in which g denotes the acceleration due to gravity. There are two characteristic wave parameters in Eq. (1), namely the angular frequency $\omega = 2\pi/T$ and the wave number $k_L = 2\pi/L$.

For relatively short waves (i.e. for small values of L/h ratio) having considerable heights with respect to water depth (i.e. for large values of H/h ratio), it is recommended to apply the nonlinear theory of waves derived by Stokes.[1] For relatively long and high waves (with large values of L/h and H/h ratios), long-wave theories should be applied, such as the cnoidal wave theory.

According to the traditional classification (see e.g. Massel 1989), an L/h ratio of about 8–10 constitutes the limit between short and long waves. An additional cue as to which theoretical wave description should be used is provided by the Ursell parameter $U_r = H/h(L/h)^2$. Wave theories based on Stokes approximations can be used for $L/h < 8$ (or even for $L/h < 10$) and for small values of the Ursell parameter (definitely for every case with $U_r < 20$). The long-wave approaches, namely cnoidal theories, ought to be used for $L/h > 10$ (or $L/h > 8$) and high U_r values. As deduced by Fenton (1979), for lower waves, there is a significant overlap between the areas of validity of Stokes and cnoidal theories, which makes it possible to choose either of these two theoretical approaches. However, although solutions from the cnoidal and Stokes theories for free surface elevations can be almost identical, the solutions for wave-induced flow velocity can differ considerably. This will be demonstrated in the following computational results.

Within the limits of applicability of the Stokes wave theory, that is, for small values of U_r and L/h, one can use the following 2nd nonlinear Stokes approximation formulas describing the water surface elevation η and the horizontal component u of the wave-induced velocity (Massel 1992):

$$\begin{gathered}\eta(x,t) = \frac{H}{2}\cos\left[2\pi\left(\frac{x}{L}-\frac{t}{T}\right)\right] + \\ \left(\frac{\pi H^2}{8L}\right)\frac{\cosh\left(\frac{2\pi h}{L}\right)}{\sinh^3\left(\frac{2\pi h}{L}\right)}\left[2+\cosh\left(\frac{4h}{L}\right)\right]\cos\left[4\pi\left(\frac{x}{L}-\frac{t}{T}\right)\right],\end{gathered} \tag{2}$$

$$\begin{gathered}u(x,z,t) = \frac{gHT}{2L}\frac{\cosh\left(\frac{2\pi(z+h)}{L}\right)}{\cosh\left(\frac{2\pi h}{L}\right)}\cos\left[2\pi\left(\frac{x}{L}-\frac{t}{T}\right)\right] + \\ \frac{3}{4}\left(\frac{\pi H}{L}\right)^2 C\frac{\cosh\left(\frac{4\pi(z+h)}{L}\right)}{\sinh^4\left(\frac{2\pi h}{L}\right)}\cos\left[4\pi\left(\frac{x}{L}-\frac{t}{T}\right)\right].\end{gathered} \tag{3}$$

The dispersion relationship for the 2nd approximation of the nonlinear Stokes wave theory has the following form (Druet 2000):

$$\left(\frac{2\pi}{T}\right)^2 = g\left(\frac{2\pi}{L}\right)\tanh\left(\frac{2\pi h}{L}\right)\left[\left(1+\frac{\pi H}{L}\right)^2 \times \frac{8+\cosh\left(\frac{8\pi h}{L}\right)}{8\sinh^4\left(\frac{2\pi h}{L}\right)}\right]. \tag{4}$$

[1] Sir George Stokes (1819-1903), Irish mathematician and physicist, worked at the University of Cambridge, dealing, among others, with fluid mechanics.

It is worth noting that the above relationship between the wave period T and length L also includes the wave height H, which is not the case for sinusoidal waves, cf. Eq. (1).

The cnoidal wave theories were rather unpopular among coastal and ocean engineers because of the elliptic functions involved, inconvenient in practical use. In order to simplify calculations, approximations have been introduced, which, however, still require some iterative procedures – for example, to find the elliptic integrals and their unknown modulus (k).

Within the cnoidal wave theory, Sobey et al (1987) presented the following formulas for the water surface elevation η and the horizontal (vertically invariable) wave-induced free stream velocity u (see Fig. 1 for notation):

$$\eta(x,t) = h_t + H\mathrm{cn}^2(x,t,k), \tag{5}$$

$$u(x,t) = \bar{u} + (gh_t)^{1/2}\left[-1 - \frac{H}{h_t\mathrm{cn}^2(x,t,k)}\left(-0.5 + k^2 - k^2\mathrm{cn}^2(x,t,k)\right)\right], \tag{6}$$

in which

$$h_t = h\left\{1 + \frac{H}{k^2 h}\left[1 - k^2 - \frac{\mathbf{E}(k)}{\mathbf{K}(k)}\right]\right\}, \tag{7}$$

$$\bar{u} = (gh_t)^{1/2}\left\{1 + \frac{H}{k^2 h_t}\left[0.5 - \frac{\mathbf{E}(k)}{\mathbf{K}(k)}\right]\right\}, \tag{8}$$

$$\mathrm{cn}^2(x,t,k) = \mathrm{cn}^2\left[2\mathbf{K}(k)\left(\frac{x}{L} - \frac{t}{T}\right); k\right]. \tag{9}$$

In the above expressions, $\mathbf{K}(k)$ and $\mathbf{E}(k)$ are complete elliptic integrals of the first and second kind, respectively, with the modulus k. The function 'cn' is a Jacobian elliptic cosine. The function 'cn' is singly periodic, provided k is a real number and $0 \leq k < 1$. The period becomes infinite when $k = 1$ (in which case we have a solitary wave). For $k = 0$, the wave is sinusoidal.

For the same as above description of the free surface elevation, Wiegel (1960) provided a more elaborate equation, yielding a velocity u variable over the elevation (y) above the bed:

$$\begin{aligned}\frac{u(x,y,t)}{(gh)^{1/2}} &= -\frac{5}{4} + \frac{3h_t}{2h} - \frac{h_t^2}{4h^2} + \left(\frac{3h}{2h} - \frac{h_t H}{2h^2}\right)\mathrm{cn}^2(x,t,k) - \frac{H^2}{4h^2}\mathrm{cn}^4(x,t,k)\\ &-\frac{8H\mathbf{K}^2(k)}{L^2}\left(\frac{h}{3} - \frac{y^2}{2h}\right)\Big[-k^2\mathrm{sn}^2(x,t,k)\mathrm{cn}^2(x,t,k) + \mathrm{cn}^2(x,t,k)\mathrm{dn}^2(x,t,k)\\ &-\mathrm{sn}^2(x,t,k)\mathrm{dn}^2(x,t,k)\Big],\end{aligned} \tag{10}$$

where 'sn' and 'dn' are two other Jacobian elliptic functions (available on the basis of 'cn' from the relations $\mathrm{sn}^2 + \mathrm{cn}^2 = 1$ and $k^2\mathrm{sn}^2 + \mathrm{dn}^2 = 1$).

In the solutions for cnoidal waves, the modulus (k) of the elliptic integrals, as well as the elliptic integrals $\mathbf{K}(k)$ and $\mathbf{E}(k)$, are unknown. The modulus k can be determined by solving the following equation (Massel 1989):

$$\left(\frac{H}{h}\right)\left(\frac{gT^2}{h}\right) = \frac{16}{3}k^2\mathbf{K}^2(k), \tag{11}$$

after which the elliptic integrals $\mathbf{K}(k)$ and $\mathbf{E}(k)$ are computed. Assuming the wave phase celerity for shallow water $C = L/T = (gh)^{1/2}$, one can rearrange Eq. (11) into the following form:

$$\left(\frac{H}{h}\right)\left(\frac{L}{h}\right)^2 = \frac{16}{3}k^2\mathbf{K}^2(k). \tag{12}$$

Eq. (12) is useful in determining the modulus k and the elliptic integral $\mathbf{K}(k)$ if the wave period T is unknown, but the wave length L is known instead.

Figures 2 and 3 show the free surface elevation calculated from Eqs. (2) and (5), the depth-invariable velocity from Eq. (6), as well as velocities at the bottom and at the wave trough from Eqs. (3) and (10).

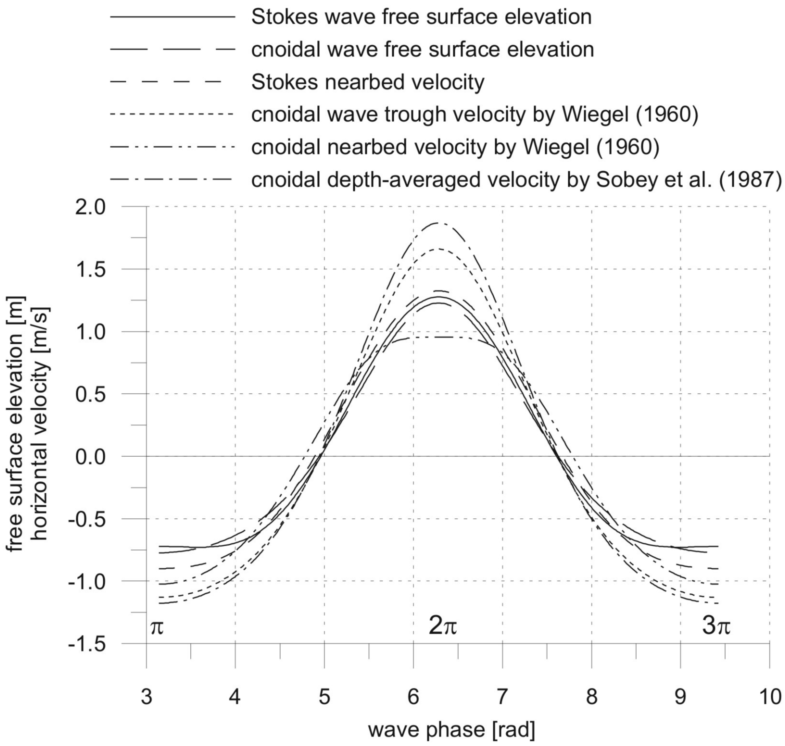

Fig. 2. Free surface elevation and wave-induced velocity obtained by various approaches for $h = 5$ m, $H = 2$ m, $T = 6$ s; $L/h \approx 8$, $U_r \approx 23$, after Ostrowski (2004)

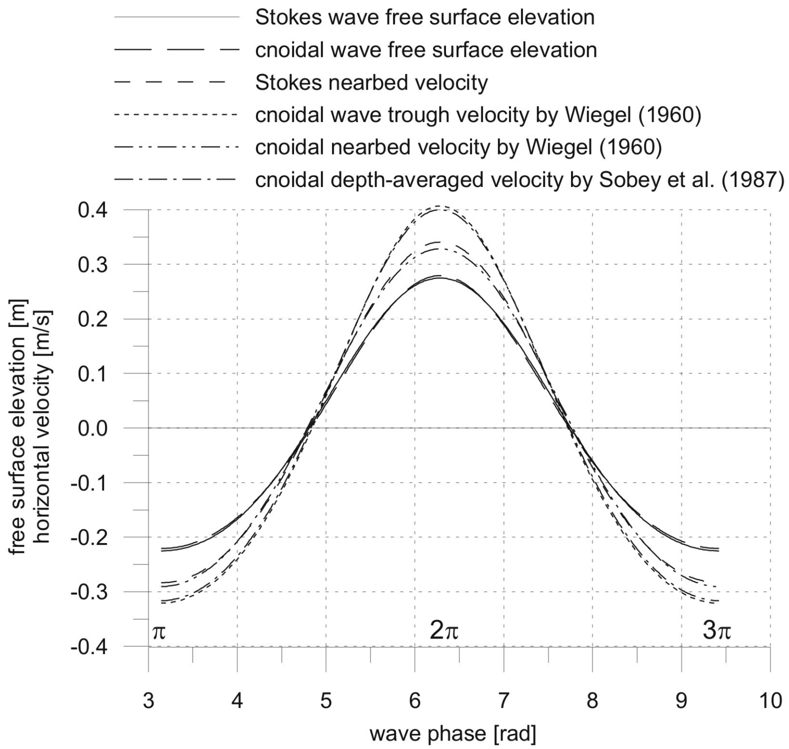

Fig. 3. Free surface elevation and wave-induced velocity obtained by various approaches for $h = 5$ m, $H = 0.5$ m, $T = 8$ s; $L/h \approx 11$, $U_r \approx 11$, after Ostrowski (2004)

It can be seen that the velocities given by Eq. (6) and Eq. (10) differ significantly from each other, particularly for large values of the H/h ratio (Fig. 2). For $H/h = 0.1$ (Fig. 3), the solution from Eq. (6) coincides with the result obtained using Eq. (10) for $y = h_t$, while the 2$^{\text{nd}}$ Stokes approximation, that is, Eq. (3), yields a velocity almost identical with that from Eq. (10) for $y = 0$.

In Fig. 2, the nearbed velocity from Eq. (10) at the wave crest phase is much less than the velocities obtained by the other solutions. To explain the above discrepancy, Ostrowski (2002, 2004) carried out computations for the conditions of laboratory experiments by Iwagaki & Sakai, as given by Fenton (1979). Tests representing long waves were chosen, with the ratio L/h changing from 9.5 to 15. The vertically invariable velocities from Eq. (6) and nearbed velocities (for $y = 0$) from Eq. (10) were calculated and superimposed on the original plots of Fenton (1979), which, aside from the abovementioned experimental data, also comprised theoretical results obtained using the 5$^{\text{th}}$ order Stokes theory and the 5$^{\text{th}}$ order cnoidal theory. This comparison with the experimental data revealed that Eq. (10) yielded the best accuracy (in all but two of the seven cases analysed). The other solutions, especially Eq. (6), overestimated the nearbed velocity at the wave crest phase. Therefore, the velocity obtained from

Eq. (10) was used in further computations of sediment transport under shallow water waves.

3. Sediment Transport under Steady Currents and Asymmetric Waves

3.1. Three-layer Sediment Transport Model

Sediment transport rates are dependent on the flow velocity u and the sediment concentration c. For stationary flows, the total sediment transport rate in a water column stretching from the bottom ($z = 0$) to the water surface ($z = h$) can be calculated using the following formula:

$$q = \int_0^h \overline{u}(z) \cdot \overline{c}(z) dz, \tag{13}$$

in which $\overline{u}(z)$ and $\overline{c}(z)$ denote time-averaged velocity and concentration, respectively.

Under conditions of unsteady flows, for example, under waves or waves combined with a steady current, the instantaneous sediment transport rate is determined as

$$q(t) = \int_0^h u(z,t) \cdot c(z,t) dz. \tag{14}$$

To determine the net (resultant) rate of sediment motion per unit width q_{net} [m^3/s/m], necessary for the modelling of sea bed morphodynamics, instantaneous transport rates ought to be integrated at each location in the coastal zone (x) over the wave period T as follows:

$$q_{net}(x) = \frac{1}{T} \int_0^T q(t)\, dt. \tag{15}$$

Sediment transport is typically divided into bedload transport, taking place just above the sea bed and reacting almost instantaneously to the local conditions, and suspended load transport, which is carried out by water motion and needs time or space to be picked up or to settle down. The suspended transport reacts indirectly to changes in flow or wave conditions through changes in the concentration field. During the motion of sandy sediments, the concentration of grains is significantly variable in the water column, from a dense water-soil mixture at the sea bed to single sand grains suspended high above the bed. Laboratory experiments and field observations have shown (see e.g. Kaczmarek and Ostrowski 2002) that sandy sediments in coastal regions are mostly subject to movement in suspension very close to the bed and in the superficial bed layer – as bedload.

As mentioned above, the concentration of sand under wave and wave-current impact is very high near the bottom. The mathematical model of bedload transport developed by Kaczmarek (1999) is based on the water-soil mixture approach, with a collision-dominated drag concept and the effective roughness height k_e (necessary for the determination of bed shear stresses). This roughness is calculated using an approximate formula presented by Kaczmarek and Ostrowski (1996). The collision-dominated granular-fluid bedload region stretches below the theoretical bed level, while the turbulent fluid region extends above it, constituting the contact load layer and the outer suspended load layer. The outer region of pure suspension is characterised by very small concentrations, where the process of sediment distribution may be considered as a convective and (or) diffusive process. In contrast, the granular-fluid region below the theoretical bed level is characterised by very high concentrations, where the inter-granular resistance is predominant. Such a three-layer sediment transport scheme, successfully applied to the modelling of coastal morphodynamics by Ostrowski (2004), is shown in Fig. 4.

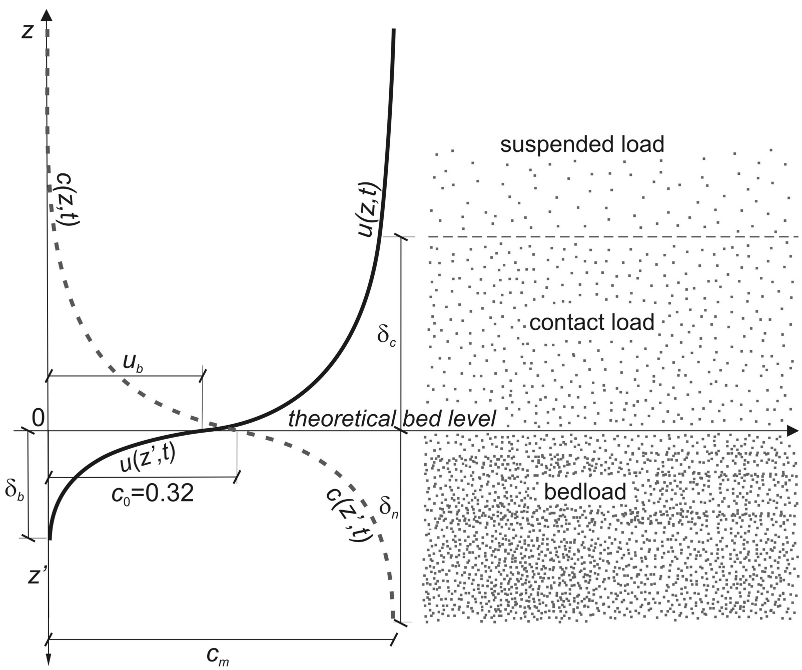

Fig. 4. Three-layer sediment transport model

According to Kaczmarek (1999), the concentration under the bedload transport layer (where sediment is not moving), at a distance of δ_n below the theoretical bed level, amounts to $c_m = 0.53$, while at the top of the bedload layer (i.e. at the lower limit of the contact load layer) it is equal to $c_0 = 0.32$. The parameter c_0 is the sediment concentration corresponding to soil fluidity, while c_m is the sediment concentration corresponding to closely packed grains and theoretically can lie in the range of 0.5–0.77.

The velocity profile in the contact load layer is assumed to be continuous. Its intersection with the nominal seabed is the apparent slip velocity u_b, identified as a characteristic velocity of sediment moving in the form of bedload.

From the hydrodynamic input, described by the nearbed wave-induced oscillatory velocities interacting with wave-driven stationary currents, the instantaneous values of bed shear stresses during a wave period are determined by the momentum integral method proposed by Fredsøe (1984), adapted for asymmetric waves by Kaczmarek (1999) and Kaczmarek and Ostrowski (2002). Then, for known shear stresses, the instantaneous bedload velocities $u(z', t)$ and concentrations $c(z', t)$ are computed (with the vertical axis z' directed downwards from the theoretical bed level, as defined in Fig. 4). The computations also yield the velocity u_b, which serves as the input into the solution of the contact load layer.

The relation between bed shear stresses (which are direct driving forces of sediment transport) and flow velocities is highly nonlinear. Therefore, although the wave-induced nearbed velocities u averaged over wave period yield zero (even for asymmetric waves), the resultant bed shear stress (and the net sediment transport rate q_{net}) is positive. This is because high velocities during the wave crest phase produce, in total, much larger shear stresses than lower velocities do during the wave trough phase (although the trough of the asymmetric wave lasts longer than its crest, see Figures 1, 2 and 3). In addition, larger shear stresses generate higher concentrations, which, on account of Eq. (14), also cause more intense sediment transport during wave crest than during wave trough transition.

The instantaneous values of the sediment transport rate are computed from distributions of velocity and concentration in the bedload layer and in the contact load layer, cf. Eq. (14):

$$q_{b+c}(t) = \int_0^{\delta_b} u(z', t) \cdot c(z', t) dz' + \int_0^{\delta_c} u(z, t) \cdot c(z, t) dz, \tag{16}$$

where δ_b is the bedload layer thickness, and δ_c denotes the upper limit of the nearbed suspension (contact load layer thickness). The quantity δ_b results from the solution of the bedload layer, while δ_c is a characteristic bottom boundary layer thickness calculated from Fredsøe's (1984) approach (see Kaczmarek and Ostrowski 2002).

The net (resultant) transport rate in the bedload and contact load layers is calculated as follows, cf. Eq. (15):

$$q_{net} = \frac{1}{T} \int_0^{T} q_{b+c}(t)\, dt. \tag{17}$$

For the outer flow, due to difficulties in accurate determination of time-dependent concentrations, the net sediment transport rate is calculated in a simplified way, using a time-averaged flow velocity and a time-averaged sediment concentration, cf. Eq. (13):

$$q_s = \int_{\delta_c}^{h} \overline{u}(z) \cdot \overline{c}(z) dz, \tag{18}$$

where the time-averaged concentration is obtained from a conventional relationship, for example, that by Ribberink and Al-Salem (1994):

$$\overline{c}(z) = \overline{c}(z = \delta_c) \left(\frac{\delta_c}{z} \right)^{\alpha}, \tag{19}$$

in which the concentration $\overline{c}(z = \delta_c)$ is found from the solution of the contact load layer.

The concentration decay parameter α is an unknown value which has to be determined, for example, from experiments. In general, it lies in the range from 1.5 to 2.1 (Ostrowski 2004), but in some cases much smaller values have been found correct, for instance, $\alpha = 0.6$ (Biegowski 2005).

3.2. Cross-shore Sediment Transport

In the quasi-phase-resolving cross-shore sediment transport model of Ostrowski (2004), the phase-averaged solution of the wave-current field in the coastal zone is followed by a detailed computation of net sediment transport rates at all locations of a cross-shore transect. In such modelling, the wave-induced nearbed velocity is described by one of two theories of asymmetric waves, depending on the regime of wave motion, indicated by the Ursell parameter $U_r = H/h(L/h)^2$ and the L/h ratio. The nearbed wave-induced velocities are combined with the undertow, and the wave-current boundary layer equations are solved, thus yielding time-dependent bed shear stresses and sediment transport rates.

The balance or imbalance between wave asymmetry and undertow can lead to various types of resultant flow (and sediment flux), as depicted in Fig. 5, in which the scheme on the left-hand side is typical of the surf zone, while the scheme on the right-hand side represents the situation farther offshore, where no wave-driven currents occur.

For the wave-current situations in Fig. 5, net sediment transport rates are calculated along the entire cross-shore profile. The sea bed profile evolution is modelled on the basis of the spatial variability of net sediment transport rates from the following continuity equation for sediment in the direction perpendicular to the shore:

$$\frac{\partial h\,(x,t)}{\partial t} = \frac{1}{1-n} \frac{\partial q_{net}\,(x,t)}{\partial x}, \tag{20}$$

where q_{net} denotes the net sediment transport rate [m^2/s] in the cross-shore direction per unit width, and n is the soil porosity while deposited.

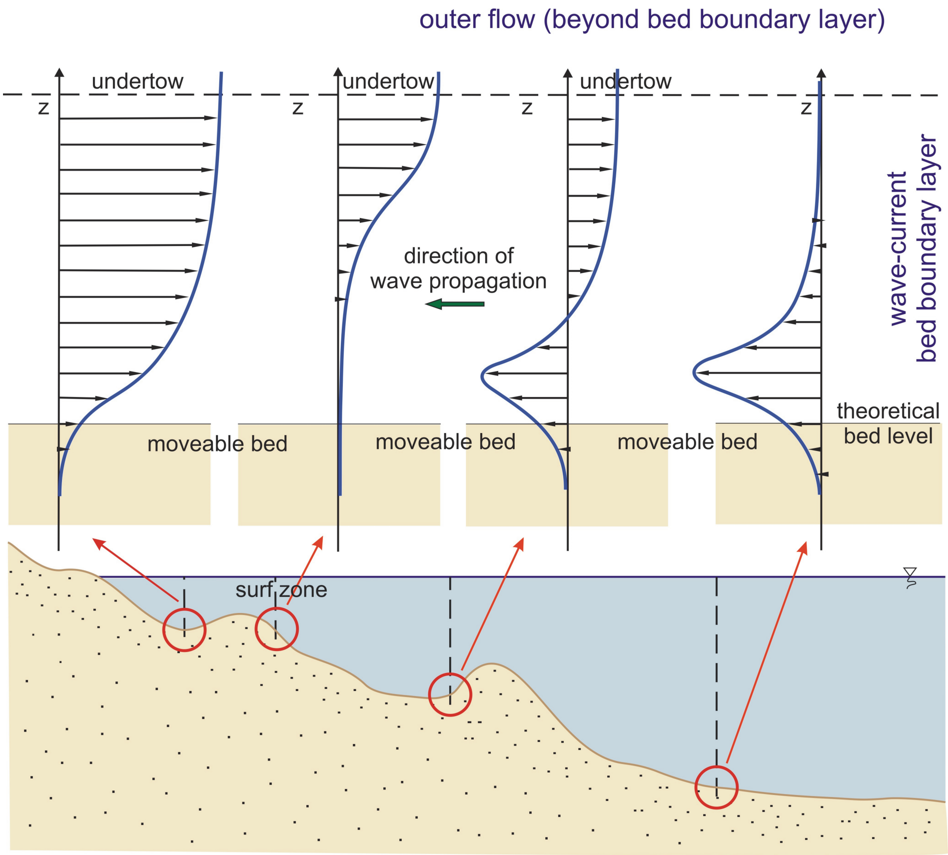

Fig. 5. Schemes of wave-current interaction in coastal bed boundary layers

Eq. (20) can be easily solved, for example, by a finite difference scheme. It is very convenient to start computations from an offshore location where there is no sediment transport, since the waves are deep-water waves, and it can be assumed that they do not affect the sea bed. Furthermore, there are no wave-driven currents at this location.

As one approaches the shore with the solution of Eq. (20), the net sediment transport due to wave asymmetry appears and increases at ever smaller water depths. Simultaneously, the undertow starts to play an increasingly important role. The undertow can become a dominant factor in the surf zone, locally causing offshore sand transport.

Fig. 6 presents the results of computations for a sea bed having a uniform slope of the cross-shore profile, with the input parameters H = 1.5 m and T = 6.5 s, median grain diameter d_{50} = 0.21 mm, settling velocity w_s = 0.026 m/s and relative density $s = \rho_s/\rho = 2.65$. The sea bed porosity was assumed as n = 0.4. Aside from the total net sediment transport rate q_{total}, all its components (namely, the bedload q_b, the contact load q_c and the suspended load q_s) determined by the three-layer sand transport model in the first time step (for an unchanged bottom) are distinguished in Fig. 6. The other results, that is, the wave height, undertow nearbed velocity and sea bed level evolution, are also presented in Fig. 6.

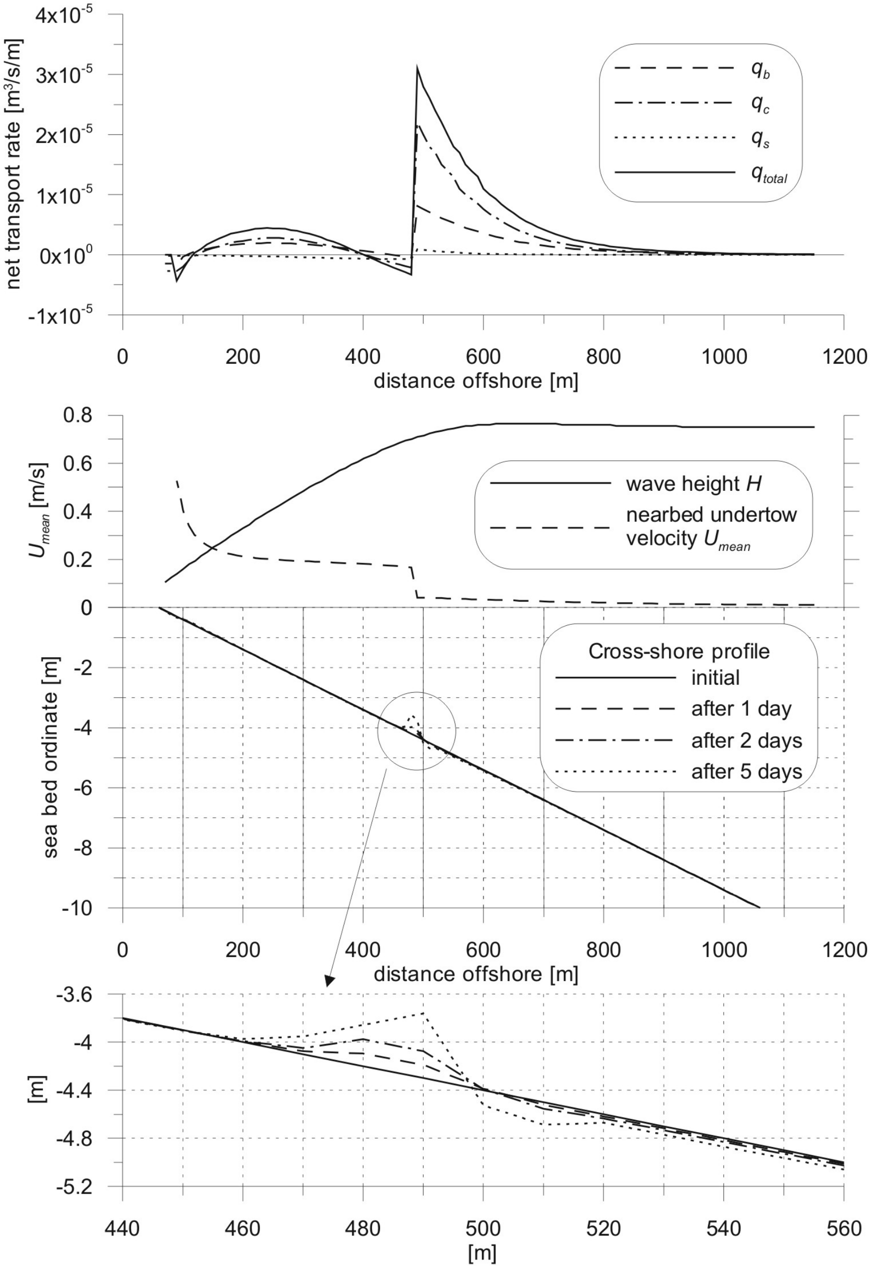

Fig. 6. Modelled hydrodynamics, net sediment transport rates and a short-term evolution of a uniformly sloped cross-shore profile, after Ostrowski (2004)

It can be seen from Fig. 6 that the nearbed undertow velocity increases very slowly landwards, reaching only a few centimetres per second before the wave breaks. Simultaneously, wave asymmetry causes a distinct increase in all sediment transport components. The suspended load transport far from the bed q_s increases as well, although it is small in comparison to the other components. The nearbed undertow velocity grows rapidly at the wave breaking point, and the undertow starts to affect the bed boundary layer. This causes great local variability (also qualitative one) in net sediment transport rates. The wave breaking point appears to be a location at which sediment fluxes converge. Further landwards, the wave motion is restored after breaking and becomes increasingly asymmetrical due to the decreasing water depth. This asymmetry effect prevails over the undertow, and the resultant sand transport is directed onshore again. Close to the shoreline, waves collapse, and the undertow velocity increases, which results in offshore-directed sediment flux. The spatial variabilities in the net transport yield the greatest sea bed changes at the location of wave breaking, which is realistic.

The net sediment transport contributions from wave asymmetry and undertow depend on site-specific conditions. In addition to the wave climate, the profile slope seems to be important. For a 1‰ slope (typical of the sandy coasts at the placeBaltic Sea), the effect of undertow can be much smaller, and the bars can "move" towards the shore even under relatively severe offshore wave conditions. For steep beaches, the situation can be different. Laboratory tests are generally carried out for beaches steeper than 1‰. However, even those laboratory data on net sand fluxes can sometimes show a much greater contribution from wave asymmetry than from undertow, see Ostrowski (2004).

3.3. Longshore Sediment Transport

As in the case of the cross-shore sediment transport, the longshore transport is assumed to depend on combined wave and current motion. This combined flow of water gives rise to a coupled bed shear stress, which is a driving force for sand movement. Under the assumptions of the present theoretical model, the motion of sediment is caused by instantaneous bed shear stresses. The instantaneous values and directions during a wave period are determined by the momentum integral method for wave-current flow, proposed by Fredsøe (1984). In the case of interaction between waves and the longshore current, the input data comprise offshore wave parameters, sea bed shape and sea bed soil parameters, the distribution of the depth-averaged longshore current velocity on the cross-shore profile and the angle of the offshore wave direction with respect to the shoreline.

The solution yields instantaneous bed shear stresses and the resultant directions of these stresses, namely the angle $\phi(\omega t)$ between the direction of the longshore current and the resultant sediment transport under wave-current impact. Next, using the angle ϕ, the instantaneous sediment transport rates $q(\omega t)$ are projected on the longshore direction, averaged over wave period, and thus the net longshore transport q_y is obtained:

$$q_y = \overline{q(\omega t) \cdot \cos\phi(\omega t)}. \tag{21}$$

The net longshore sediment transport determined from Eq. (21) requires a complete solution of the bedload and contact load layers, as well as higher above them, in the same way as in the case of the cross-shore transport.

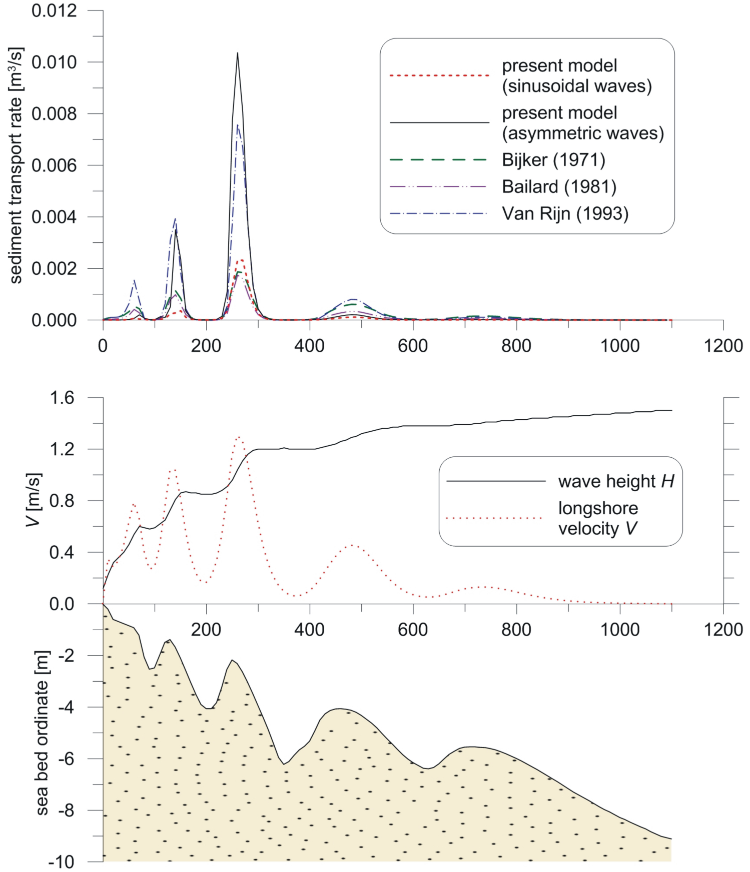

Fig. 7. Cross-shore profile of the sea bed at CRS Lubiatowo with wave heights, longshore flow velocities, longshore sediment transport rate distributions determined by the present model for sinusoidal and asymmetric waves, as well as the models of Bijker (1971), Bailard (1981) and Van Rijn (1993) for the following incoming wave parameters: $H = 1.5$ m, $T = 6$ s and $\theta = 45°$

The model was run for a typical bathymetric cross-shore profile measured at the IBW PAN Coastal Research Station (CRS) at Lubiatowo. The profile was about 1100 m long and had a depth of more than 9 m on its offshore boundary, thus covering the entire coastal zone with 4 distinct bars, as shown in Fig. 7. The input parameters were as follows: H = 1.5 m, T = 6 s, wave approach angle (angle between the wave ray and the cross-shore direction) $\theta = 45°$, median grain diameter d_{50} = 0.21 mm, settling velocity w_s = 0.026 m/s and relative density $s = \rho_s/\rho = 2.65$. The offshore wave parameters correspond to typical moderate storm conditions at the south Baltic coast. The hydrodynamic outputs of the model, that is, the variability of wave height and longshore flow velocity on the cross-shore profile, are also shown in Fig. 7, together with the distribution of longshore sediment transport rates on the cross-shore transect determined by the present modelling system for symmetric (sinusoidal) and asymmetric waves, as well as – for comparison – the rates determined by the sediment transport models of Bijker (1971), Bailard (1981) and Van Rijn (1993).

It can be seen in Fig. 7 that the present modelling results lie below the other solutions, except for locations 230–310 m offshore (at the second bar), where the present model for asymmetrical waves gives the highest rates. At the other cross-shore locations, Van Rijn's (1993) approach yields higher rates than all other models.

The results for sinusoidal and asymmetrical waves obtained using the present model and presented in Fig. 7 clearly show that the asymmetrical wave shape causes a significant increase in sediment transport rate.

A detailed analysis of the computational results shown in Fig. 7 reveals a highly nonlinear relationship between the hydrodynamic input and the sediment transport rates. The results from all models considered here show that most of the longshore sediment transport is concentrated in a relatively narrow zone near the major wave breaker, where high waves are accompanied by a strong longshore flow. This effect is most pronounced in the present model.

4. Final Remarks and Conclusions

The process of sediment transport is highly non-linear with respect to water flow, which is its driving force. Because of flow patterns produced by wave motion, sediment moves with the wave or against the wave during the phases of wave crest and trough, respectively. The net transport results from differences in the wave shape during these phases, which occur for asymmetric waves. Although the mean velocity for such waves at any ordinate above the sea bed amounts to zero, the nearbed net transport is always directed accordingly to wave propagation because of non-linear effects. Roughly, due to these effects, more sand is transported at wave crest than at wave trough. Obviously, this concerns only the purely wave-induced sediment motion. The presence of wave-driven currents, such as undertow, can be significant, causing sediment to move against the wave.

As proved by the computations, the net sediment transport rate is highly sensitive to changes in nearbed wave-induced velocities. A correct description of the nearbed free stream velocity, namely its distribution over the wave period, is necessary for precise prediction of sediment transport. To that end, the cnoidal and Stokes approaches can be used within their ranges of applicability. However, further theoretical and experimental studies would be needed to verify the accuracy of the modelling of nearbed wave-driven flows. These studies should investigate free stream velocities caused not only by vertically asymmetric waves (with short high crests and long shallow troughs), but also by horizontally asymmetric waves (with a steep front of the crest and a mildly inclined back of the crest).

The results of the present study can be helpful in formulation of a complex quasi-phase-resolving coastal sediment transport model. In the enhanced model, any classical solution of the wave-current field in the coastal zone ought to be followed by the computation of resultant sediment transport rates at all locations of the coastal zone. Consequently, sea bed profile evolution can be modelled. Within such an approach, the wave-induced nearbed velocity will be described using various wave theories, depending on the regime of wave motion identified by the Ursell parameter and the L/h ratio, as well as by other features. The proposed modelling method does not exclude more sophisticated approaches, namely fully phase-resolving models applied to the entire coastal regions, using the present sediment transport module. If any of the above concepts are successful, the sediment transport module can be used in a three-dimensional model, providing a reliable means of predicting coastal changes simultaneously in the cross-shore and longshore directions.

Acknowledgements

The study was sponsored by the Ministry of Science and Higher Education of Poland under mission-related programme No. 2 of the Institute of Hydro-Engineering of the Polish Academy of Sciences.

References

Bailard J. A. (1981) An energetics total load sediment transport model for a plane sloping beach, *Journal of Geophysical Research*, **86**, (C11), 10938–10954.

Biegowski J. (2005) Dynamics of graded marine sediments in view of theory and experiment, *PhD Thesis*, IBW PAN Publishers, Gdańsk, pp. 123 (in Polish).

Bijker E. W. (1971) Longshore Transport Computations, *Journal of Waterways, Harbour and Coastal Engineering*, **99**, (WW4), 687–701.

Druet C. (2000) *Sea Dynamics*, Wydawnictwo Uniwersytetu Gdańskiego oraz Gdańskie Towarzystwo Naukowe, Gdańsk, pp. 288 (in Polish).

Fenton J. D. (1979) A high-order cnoidal wave theory, *J. Fluid Mech.*, **94**, (1), 129–161.

Fredsøe J. (1984) Turbulent boundary layer in combined wave-current motion, *J. Hydraulic country-regionplaceEng.*, ASCE, **110**, (HY8), 1103–1120.

Kaczmarek L. M. (1999) Moveable Sea Bed Boundary Layer and Mechanics of Sediment Transport, *DSc Thesis*, IBW PAN Publishers, Gdańsk, ISBN 83-85708-35-9, pp. 209.

Kaczmarek L. M., Ostrowski R. (1996) Bedload Under Asymmetric and Irregular Waves: Theory Versus Laboratory Data, *Archives of Hydro-Engineering and Environmental Mechanics*, **43**, (1–4), 21–42.

Kaczmarek L. M., Ostrowski R. (2002) Modelling intensive near-bed sand transport under wave-current flow versus laboratory and field data, *Coastal Engineering*, Elsevier Science B.V., **45**, (1), 1–18.

Massel S. R. (1989) *Hydrodynamics of coastal zones*, Elsevier Oceanography Series, Elsevier Science, Amsterdam, pp. 335.

Massel S. R. (1992) Waves in unconfined and confined basins, [in:] *Poradnik hydrotechnika*, ed. Massel S. R., Wydawnictwo Morskie Gdańsk, pp. 338 (in Polish).

Ostrowski R. (2002) Application of cnoidal wave theory in modelling of sediment transport, *Archives of Hydro-Engineering and Environmental Mechanics*, **49**, (1), 107–118.

Ostrowski R. (2003) A quasi phase-resolving model of net sand transport and short-term cross-shore profile evolution, Oceanologia, **45**, (2), 261-282.

Ostrowski R. (2004) Morphodynamics of a Multi-Bar Coastal Zone, *DSc Thesis*, IBW PAN Publishers, Gdańsk, ISBN 83-85708-64-2, pp. 163.

Ostrowski R., Szmytkiewicz M. (2006) Modelling longshore sediment transport under asymmetric waves, *Oceanologia*, **48**, (3), 395–412.

Ribberink J. S., Al-Salem A. (1994) Sediment transport in oscillatory boundary layers in cases of rippled beds and sheet flow, *Journal Geoph. Res.*, **99**, (C6), 12707–12727.

Sobey R. J., Goodwin P., Thieke R. J., Westberg R.J. (1987) Application of Stokes, cnoidal and Fourier wave theories, *J. Waterway, Port, Coastal and Ocean Engineering*, **113**, (6), 565–587.

Szmytkiewicz M. (1996) 2D velocity distributions in nearshore currents, *Proc. Coastal Dynamics'95*, ASCE, New York, 366–376.

Szmytkiewicz M. (2002a) Wave-induced currents in the coastal zone, *DSc Thesis*, IBW PAN Publishers, Gdańsk, ISBN 83-85708-45-6, pp. 235 (in Polish).

Szmytkiewicz M. (2002b) Quasi 3D model of wave-induced currents in coastal zone, *Archives of Hydro-Engineering and Environmental Mechanics*, **49**, (1), 57–81.

Van Rijn L. C. (1993) Principles of sediment transport in rivers, estuaries and coastal seas, *Aqua Publications*, Amsterdam, pp. 614.

Wiegel R. L. (1960) A presentation of cnoidal wave theory for practical application, *J. Fluid Mech.*, **7**, 273–286.